

## High efficiency electrospun TiO<sub>2</sub> nanofiber based hybrid organic-inorganic perovskite solar cell.

Sabba Dharani<sup>1,2</sup>, Hemant Kumar Mulmudi<sup>1,2</sup>, Natalia Yantara<sup>1,2</sup>, Pham Thi Thu Thrang<sup>1,2</sup>, Nam Gyu Park<sup>3</sup>, Michael Graetzel<sup>4</sup>, Subodh Mhaisalkar<sup>1,2</sup>, Nripan Mathews<sup>1,2,5\*</sup>, Pablo P. Boix<sup>1\*</sup>.

1. Energy Research Institute @NTU (ERI@N), Research Techno Plaza, X-Frontier Block, Level 5, 50 Nanyang Drive, Singapore 637553.
2. School of Materials Science and Engineering, Nanyang Technological University, Nanyang Avenue, Singapore 639798.
3. School of Chemical Engineering and Department of Energy Science, Sungkyunkwan University, Suwon 440-746, Korea.
4. Laboratory of Photonics and Interfaces, EPFL, Lausanne, Switzerland.
5. Singapore-Berkeley Research Initiative for Sustainable Energy, 1 Create Way, Singapore 138602, Singapore.

\* Correspondence to: [Nripan@ntu.edu.sg](mailto:Nripan@ntu.edu.sg), [PBPablo@ntu.edu.sg](mailto:PBPablo@ntu.edu.sg)

### Supporting Information

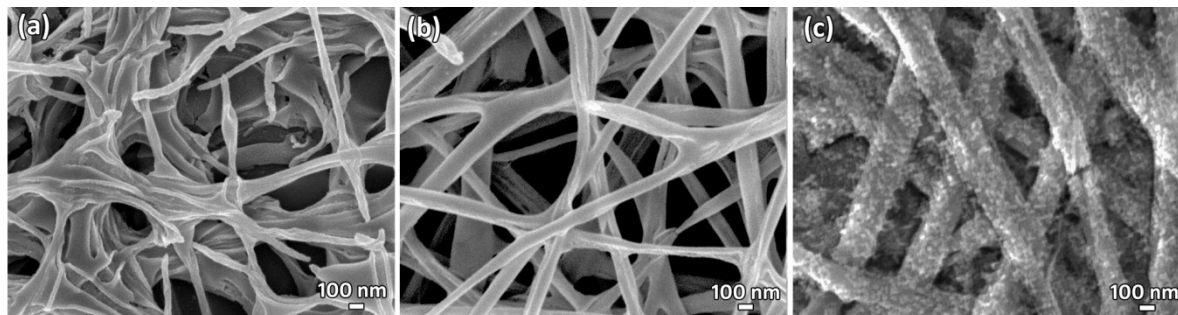


Fig. S1: FESEM images showing: (a) small diameter and discontinuous nanofibers, (b) optimized diameter and continuous nanofibers and (c) nanofibers with large diameter but with closed pores, for similar electrospinning times.

The various morphologies of the nanofibers can be attained by varying extrinsic electrospinning parameters which include applied voltage, solution feed-rate, distance travelled by the solution to reach the substrate and solution viscosity. When the solution is diluted and is electrospun at 25 kV, with a feed-rate of 0.1 mL/h, the electrospun nanofibers are thin but are discontinued as shown in Fig. S1 (a). Upon increasing the solution viscosity and with voltage of 25 kV and feed-rate of 0.3 mL/h, the

nanofibers are less broken and the pores between them are more pronounced (Fig. S1 b). If the viscosity of the solution is further enhanced, with higher feed-rate of 0.5 mL/h and voltage of 18 kV, the diameter of the nanofibers increases which leads to reduction in pores in-between the nanofibers, as seen in Fig. S1 (c). When the solution viscosity changes, it is essential to change other parameters like feed-rate and voltage to acquire required shape and size of the nanofibers.

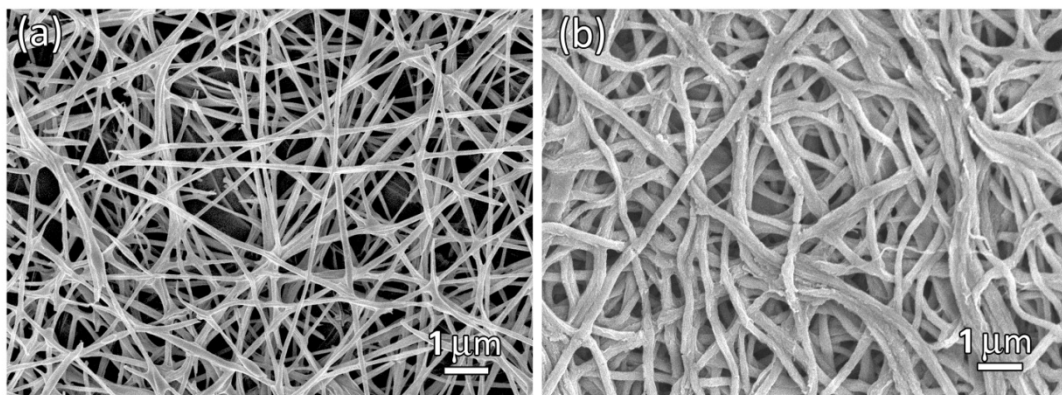


Fig. S2: FESEM image showing top-view of nanofiber films: (a) electrospun for a shorter time resulting in a porous network, (b) electrospun for longer time resulting in a thicker film with closed pores.

Fig. S2, shows the FESEM images illustrating the effect of electrospinning time on the pore-distribution. When the electrospinning is done for less time (7.5 Min), thinner mat of nanofibers is obtained with the nanofibers spread all over and revealing pores in-between them. If the electrospinning time is increased to 15 Min, then there is a higher density of nanofibers leading to overlapping and thereby reducing the pores in-between them.

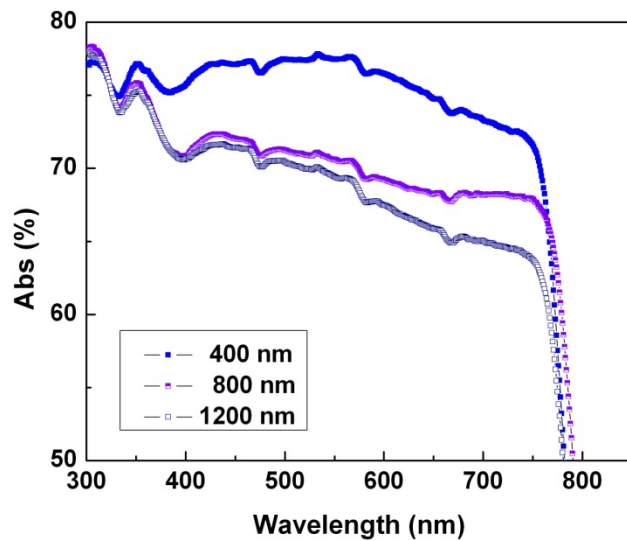


Fig. S3: Effect of different nanofiber film thickness on absorption of light.

Fig. S3, shows that as the nanofiber film thickness increased the amount of light absorbed decreased. This supports our claim that as the film thickness increases, the pores between the fibers are closed leading to lower amount of perovskite loading which inturn attributes to the lower absorption of light.

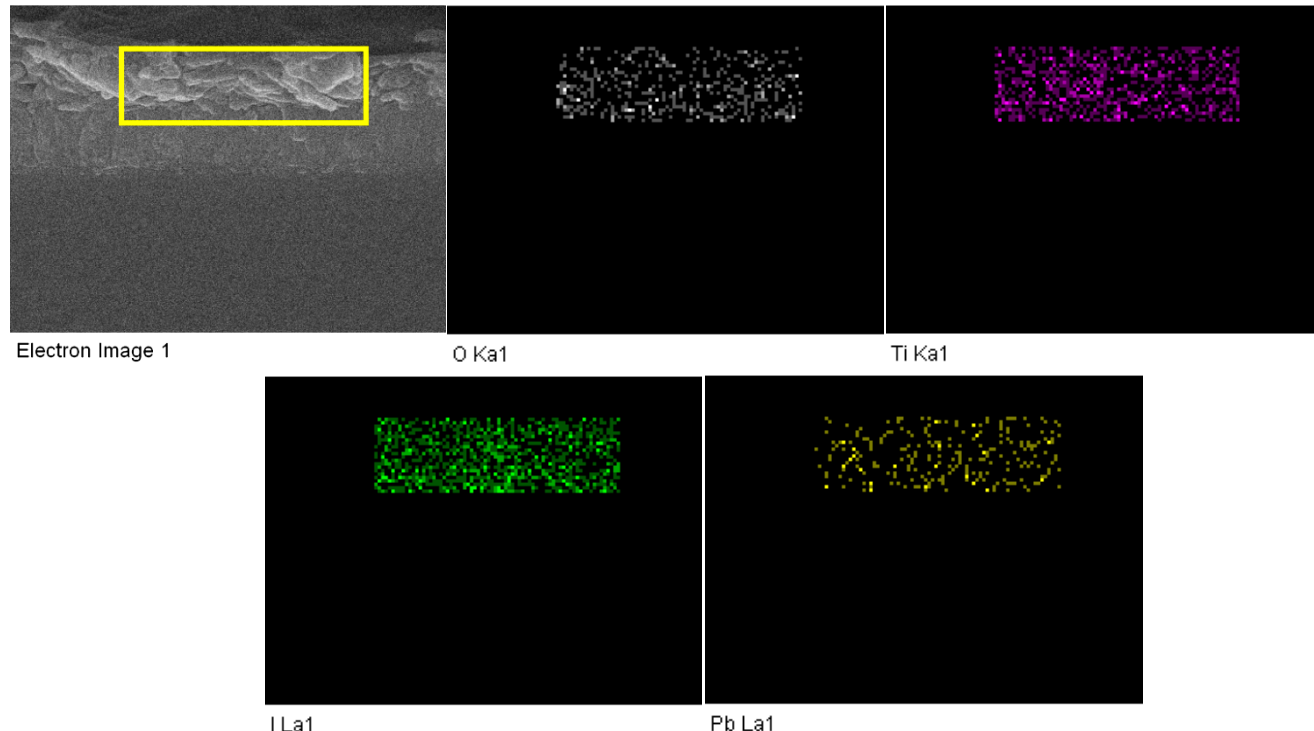


Fig: S4 EDX mapping in SEM along the nanofiber film thickness to show the distribution of Pb, I, Ti, O inside  $\text{PbI}_2$  loaded  $\text{TiO}_2$  nanofiber layer.

The EDX mapping of the cross-section area enclosed within the yellow rectangle shows the distribution of various elements: O, Ti, I and Pb along the nanofiber film thickness. It is evident from the EDX mapping that  $\text{PbI}_2$  was able to infiltrate the entire nanofiber film owing to the open pores of the nanofiber network. The large pores of the nanofiber network facilitate easy infiltration of  $\text{PbI}_2$  till the base of the film.

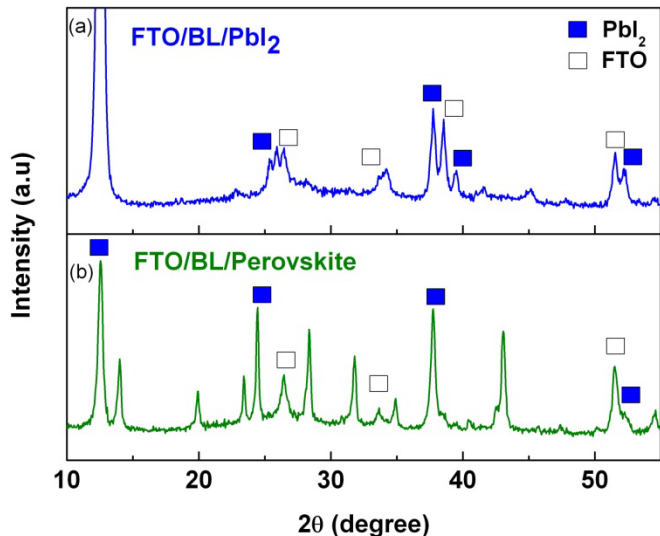


Fig: S5 XRD spectra of planar device with (a)  $\text{PbI}_2$  spincoated on FTO with blocking layer (BL) and (b) perovskite which was formed after immersing the  $\text{PbI}_2$  spincoated sample in IPA solution containing  $\text{CH}_3\text{NH}_3\text{I}$ .

The XRD spectra have been recorded for planar samples with the following configuration: FTO/blocking layer/  $\text{PbI}_2$  or  $\text{CH}_3\text{NH}_3\text{PbI}_3$ . In Fig. S4, the diffraction peaks marked by blue squares represent the  $\text{PbI}_2$  peaks and conforms well to the literature data.[1, 2] The peaks marked by open squares originate from the FTO substrate. In Fig. S4 (b), additional diffraction peaks (left unmarked) are observed upon reacting the  $\text{PbI}_2$  coated substrates with  $\text{CH}_3\text{NH}_3\text{I}$  which is due to the formation of  $\text{CH}_3\text{NH}_3\text{PbI}_3$  perovskite.[1, 2] The presence of  $\text{PbI}_2$  peaks even after exposure of the  $\text{PbI}_2$  coated planar substrate to  $\text{CH}_3\text{NH}_3\text{I}$  clearly indicates that the transformation to  $\text{CH}_3\text{NH}_3\text{PbI}_3$  perovskite is incomplete.

## References

1. Baikie, T., et al., *Synthesis and crystal chemistry of the hybrid perovskite  $(\text{CH}_3\text{NH}_3)\text{PbI}_3$  for solid-state sensitised solar cell applications*. Journal of Materials Chemistry A, 2013. **1**(18): p. 5628-5641.
2. Burschka, J., et al., *Sequential deposition as a route to high-performance perovskite-sensitized solar cells*. Nature, 2013.